

Imaging of Fluorescent Protein Activity in Mice with Multispectral Optoacoustic Tomography (MSOT)

Nikolaos C. Deliolanis, Adrian Taruttis, Amir Rosenthal, Daniel Razansky, Vasilis Ntziachristos
Institute for Biological and Medical Imaging, Technical University of Munich and Helmholtz Center Munich, Munich Germany

Author e-mail address: n.deliolanis@helmholtz-muenchen.de

Abstract: The use of the newly discovered Red-Shifted Fluorescent Proteins (FPs) is exploited in Multispectral Optoacoustic Tomography (MSOT). Analysis and phantom experiments show the great potential of this method to image FPs in murine models.

©2009 Optical Society of America

OCIS codes: (170.6280) Spectroscopy, fluorescence and luminescence; (170.6960) Tomography; (170.3010) Image reconstruction techniques

1. Introduction

Fluorescent proteins (FPs) have emerged as a very powerful imaging tool in biomedical research. The introduction of transgenes that encode fluorescent proteins into cells has enabled the visualization of biological processes and imaging of transcription, protein function and cell trafficking non-invasively and in-vivo [1]. FPs have been used in numerous applications such as cancer and stem cell research [2], immunology [3], and drug discovery [4].

So far fluorescent proteins have been used in traditional fluorescence imaging modalities, such as microscopy and its variants (intravital, confocal, two photon microscopy etc.). However penetration and imaging depth is limited up to 0.5 mm. Traditional macroscopic small animal imaging utilizing a photographic lens and a camera can record fluorescence activity coming from much deeper areas, but in expense of resolution due to the high scattering from tissue. Application examples span in the area of cancer metastasis [5], angiogenesis, and monitoring cancer progression and treatment efficiency. More recently transillumination imaging, have showed increased performance [6] especially when used in conjugation with tomographic reconstructions of 3D images of the fluorescence activity inside the tissue [7].

The most commonly used proteins is Green Fluorescent Protein (GFP) together with its mutation variants that have similar optical properties like Cyan FP (CFP) and Yellow FP (YFP). These FPs emit in the visible spectrum range below the optical absorption barrier of 600nm, and their fluorescence signals are highly attenuated, making deep tissue imaging and tomography a difficult task. But the development of a new generation of fluorescent proteins [8-11] operating in the near red part of the spectrum open combined with the use of appropriate excitation wavelengths can enable deep tissue imaging similarly to the near-infrared fluorescent probes [12, 13].

Optoacoustic tomography (OT) is an emerging imaging technology, where the object is illuminated with short laser pulses that are absorbed by tissue and thermally produce ultrasound pulses. The photoacoustic signals are recorded from different angles and are used to tomographically reconstruct the 3D distribution of the absorption in the object. It was recently shown that optoacoustic tomography can resolve fluorophore concentration in mouse tissue by multispectral data acquisition and processing [14]. Every fluorophore has a known absorption spectral profile that can be fitted to unmix it from the background absorption.

In this paper we compare the performance of the most promising fluorescent proteins for use in MSOT, a) with a simple photon propagation model and b) with an experiment imaging a tissue mimicking phantom.

2. Theoretical photon propagation model and calculations

In order to predict the performance of the fluorescent proteins in deep tissue imaging, we employ a simple photon propagation model for transillumination imaging. We assume that an excitation beam at wavelength λ_1 with intensity I_o enters the tissue and that is propagated until it reaches and excites the fluorescent protein (Fig 1). The intensity after propagating at x depth is $I_x = T(x, \lambda_1)I_o$, where $T(x, \lambda_1)$ is the relative spectral transmittance of tissue for thickness x at wavelength λ_1 . The photoacoustic signal amplitude is $I_m \propto (1 - \Phi)\epsilon I_x$, where ϵ is the molar extinction coefficient and Φ the quantum yield of the FP. So the intensity of the photoacoustic signal emitted from the fluorescent protein is:

$$I_m \approx (1 - \Phi) \varepsilon T(x, \lambda_1) I_o. \quad (1)$$

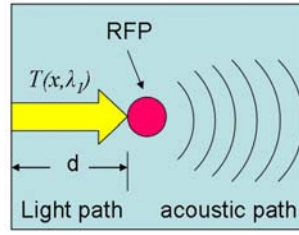


Fig. 1. Theoretical photon propagation model

We have calculated the emanating photoacoustic signal intensity of tdTomato, mPlum, mCherry, mRaspberry, dsRed, Katushka, mKate2, and 70% oxygenated hemoglobin itself, for typical deep tissue geometry where the light propagation path length is $x=0.8$ cm (Fig. 2). We used the optical properties of the fluorescent proteins as reported in the literature [8-11], and we measured the spectral transmission properties of 0.8 cm thick mouse tissue using a spectrophotometer in transillumination geometry.

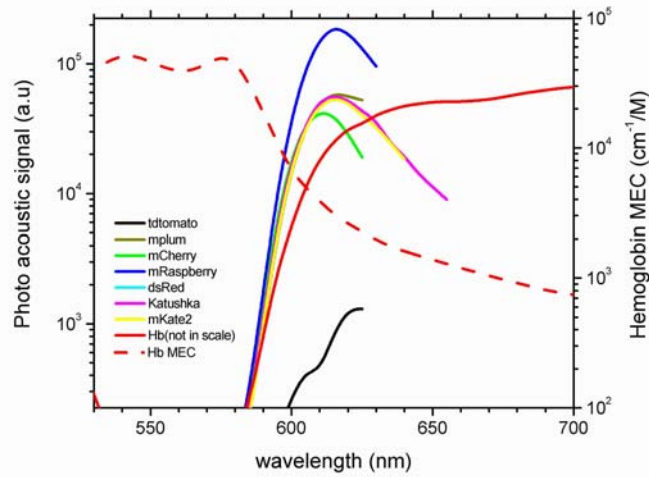


Fig. 2. Photoacoustic signal intensity emanating from deep tissue of the most promising FPs vs wavelength. The photoacoustic signal of the hemoglobin itself is plotted as well, but not in scale. For reference the absorption spectrum of 70% oxygenated hemoglobin is presented.

According to the calculations the fluorescent protein with the strongest photoacoustic signal for this particular deep tissue imaging geometry is mRaspberry, which is almost three times as strong compared to the mPlum, dsRed, Katushka, and mKate2. On the contrary, for deep tissue fluorescence imaging it is Katushka that is twice as bright compared to mRaspberry [15]. The reason for this opposite behavior is that Katushka (and mKate) do not have an excitation maximum as red shifted as mRaspberry and they have lower molar extinction coefficient.

3. Experiments with tissue mimicking phantom.

In order to demonstrate the feasibility of MSOT to image fluorescence proteins we created and imaged a tissue mimicking phantom. It was made with agar, 1% intralipid (as a scattering medium) and 3% whole blood as a scatterer giving a background absorption of 0.5 cm^{-1} at 615 nm. The phantom had two cylindrical inclusions, one was a control having the same content as the bulk, and the second one had additionally $2 \mu\text{M}$ of Texas Red (that simulates the emission spectrum of the red fluorescent proteins) adding approximately 0.05 cm^{-1} at 615 nm. Typical reconstructions using a back-projection algorithm [14, 16] for 610, 620, and 630 nm are presented in Fig 3. In the lower right corner appears the TexasRed inclusion, and on the upper left the control inclusion has the same absorption value as the background. The Texas Red to background absorption ratio was calculated to be 1.21, 1.26, and 1.30 for the 630, 620, and 610 nm. The ratio is increasing with decreasing wavelengths as expected from Fig 2.

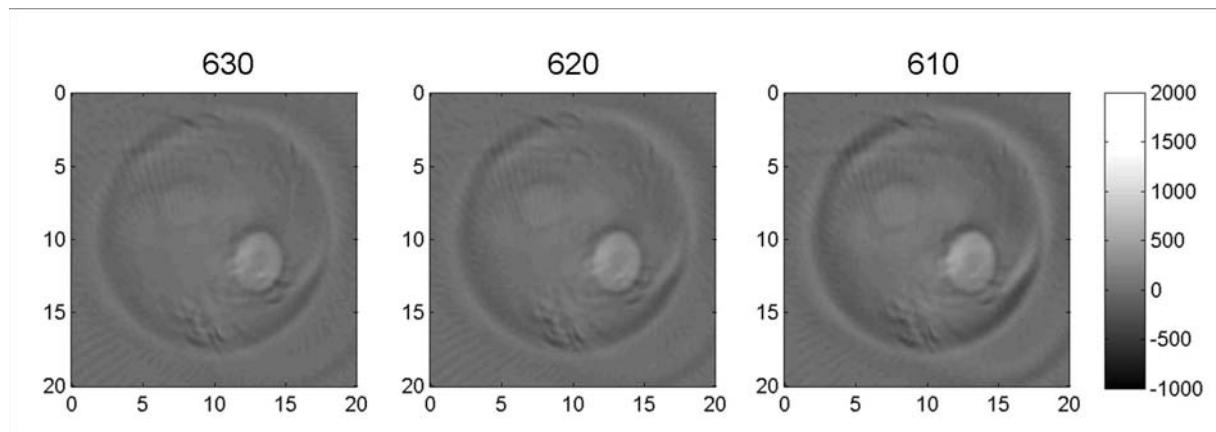


Fig. 3. Deep tissue imaging experiment a) position of the FP tube, b) fluorescence signal from mCherry, and intensity signal from GFP, tdTomato and mCherry fluorescent proteins, respectively, vs emission wavelength (points-experimental data, lines-theoretical model). The presented size scale is in mm.

4. Discussion

In this paper we demonstrate the feasibility to image fluorescent proteins with MSOT by an analytical study and simulation experiments with tissue mimicking phantoms. Comparative analysis of the fluorescent proteins shows that mRaspberry is the best choice, not only because it can produce 3 times stronger signal compared to any other available fluorescent protein at the moment, but also has a much steeper absorption drop above 615, which can be easily separated from the hemoglobin absorption in MSOT. Additionally, mRaspberry is also an excellent choice for fluorescence imaging, since only Katushka is twice as bright in deep tissue imaging [15].

5. Acknowledgements

This research is supported by a Marie Curie Intra-European Fellowship within the 7th European Community Framework.

6. References

- [1] C. H. Contag, D. Jenkins, F. R. Contag, and R. S. Negrin, "Use of reporter genes for optical measurements of neoplastic disease in vivo," *Neoplasia* **2**, 41-52 (2000).
- [2] K. Shah, A. Jacobs, X. O. Breakefield, and R. Weissleder, "Molecular imaging of gene therapy for cancer," *Gene Ther.* **11**, 1175-1187 (2004).
- [3] A. Griekspoor, W. Zwart, and J. Neefjes, "Presenting antigen presentation in living cells using biophysical techniques," *Curr. Opin. Microbiol.* **8**, 338-343 (2005).
- [4] K. Licha, and C. Olbrich, "Optical imaging in drug discovery and diagnostic applications," *Advanced Drug Delivery Reviews* **57**, 1087-1108 (2005).
- [5] H. Kishimoto, T. Kojima, Y. Watanabe, S. Kagawa, T. Fujiwara, F. Uno, F. Teraishi, S. Kyo, H. Mizuguchi, Y. Hashimoto, Y. Urata, N. Tanaka, and T. Fujiwara, "In vivo imaging of lymph node metastasis with telomerase-specific replication-selective adenovirus," *Nat. Med.* **12**, 1213-1219 (2006).
- [6] G. Zacharakis, H. Shih, J. Ripoll, R. Weissleder, and V. Ntziachristos, "Normalized transillumination of fluorescent proteins in small animals," *Mol. Imaging* **5**, 153-159 (2006).
- [7] G. Zacharakis, H. Kambara, H. Shih, J. Ripoll, J. Grimm, Y. Saeki, R. Weissleder, and V. Ntziachristos, "Volumetric tomography of fluorescent proteins through small animals in vivo," *Proc. Natl. Acad. Sci. U. S. A.* **102**, 18252-18257 (2005).
- [8] N. C. Shaner, R. E. Campbell, P. A. Steinbach, B. N. G. Giepmans, A. E. Palmer, and R. Y. Tsien, "Improved monomeric red, orange and yellow fluorescent proteins derived from *Discosoma* sp red fluorescent protein," *Nat. Biotechnol.* **22**, 1567-1572 (2004).
- [9] D. Shcherbo, E. M. Merzlyak, T. V. Chepurnykh, A. F. Fradkov, G. V. Ermakova, E. A. Solovieva, K. A. Lukyanov, E. A. Bogdanova, A. G. Zaraisky, S. Lukyanov, and D. M. Chudakov, "Bright far-red fluorescent protein for whole-body imaging," *Nat. Methods* **4**, 741-746 (2007).
- [10] L. Wang, W. C. Jackson, P. A. Steinbach, and R. Y. Tsien, "Evolution of new nonantibody proteins via iterative somatic hypermutation," *Proc. Natl. Acad. Sci. U. S. A.* **101**, 16745-16749 (2004).
- [11] D. Shcherbo, C. S. Murphy, G. V. Ermakova, E. A. Solovieva, T. V. Chepurnykh, A. S. Shcheglov, V. V. Verkhusha, V. Z. Pletnev, K. L. Hazelwood, P. M. Roche, L. Lukyanov, A. G. Zaraisky, M. W. Davidson, and D. M. Chudakov, "Far-red fluorescent tags for protein imaging in living tissues," *Biochem. J.*, (2009-in press).
- [12] R. Weissleder, C. H. Tung, U. Mahmood, and A. Bogdanov, "In vivo imaging of tumors with protease-activated near-infrared fluorescent probes," *Nat. Biotechnol.* **17**, 375-378 (1999).
- [13] M. Gurfinkel, S. Ke, X. X. Wen, C. Li, and E. M. Sevick-Muraca, "Near-infrared fluorescence optical imaging and tomography," *Dis. Markers* **19**, 107-121 (2003-2004).
- [14] D. Razansky, C. Vinegoni, and V. Ntziachristos, "Multispectral photoacoustic imaging of fluorochromes in small animals," *Opt. Lett.* **32**, 2891-2893 (2007).
- [15] N. C. Delioulis, R. Kasmieh, T. Wurdinger, B. A. Tannous, K. Shah, and V. Ntziachristos, "Performance of the red-shifted fluorescent proteins in deep-tissue molecular imaging applications," *J. Biomed. Opt.* **13**, 9 (2008).
- [16] X. D. Wang, Y. J. Pang, G. Ku, X. Y. Xie, G. Stoica, and L. H. V. Wang, "Noninvasive laser-induced photoacoustic tomography for structural and functional in vivo imaging of the brain," *Nat. Biotechnol.* **21**, 803-806 (2003).

